DOI: 10.1534/genetics.104.033399

MLH1 and *MSH2* Promote the Symmetry of Double-Strand Break Repair Events at the *HIS4* Hotspot in *Saccharomyces cerevisiae*

Eva R. Hoffmann, Emma Eriksson, Benjamin J. Herbert and Rhona H. Borts[1]

Department of Genetics, University of Leicester, Leicester LE1 7RH, United Kingdom

Manuscript received July 9, 2004
Accepted for publication December 6, 2004

ABSTRACT

Double-strand breaks (DSBs) initiate meiotic recombination. The DSB repair model predicts that both genetic markers spanning the DSB should be included in heteroduplex DNA and be detectable as non-Mendelian segregations (NMS). In experiments testing this, a significant fraction of events do not conform to this prediction, as only one of the markers displays NMS (one-sided events). Two explanations have been proposed to account for the discrepancies between the predictions and experimental observations. One suggests that two-sided events are the norm but are "hidden" as heteroduplex repair frequently restores the parental configuration of one of the markers. Another explanation posits that one-sided events reflect events in which heteroduplex is formed predominantly on only one side of the DSB. In the absence of heteroduplex repair, the first model predicts that two-sided events would be revealed at the expense of one-sided events, while the second predicts no effect on the distribution of events when heteroduplex repair is lost. We tested these predictions by deleting the DNA mismatch repair genes *MSH2* or *MLH1* and analyzing the proportion of two-sided events. Unexpectedly, the results do not match the predictions of either model. In both *mlh1*Δ and *msh2*Δ, the proportion of two-sided events is significantly decreased relative to wild type. These observations can be explained in one of two ways. Either Msh2p/Mlh1p-independent mispair removal leads to restoration of one of the markers flanking the DSB site or Msh2p/Mlh1p actively promote two-sided events.

THE double-strand break (DSB) repair model proposed by Szostak *et al.* (1983) predicts that heteroduplex DNA is formed on both sides of the DSB (Figure 1). Thus, when resection, strand invasion, and strand capture include markers placed on opposite sides of the DSB, both markers should show non-Mendelian segregation (NMS; Schultes and Szostak 1990; Figure 1). Such events have been termed "two-sided" events. However, other genetic evidence suggests that "one-sided" events are common and that the proportion thereof may be hotspot specific (Schultes and Szostak 1990; Porter *et al.* 1993; Gilbertson and Stahl 1996; Merker *et al.* 2003; Jessop *et al.* 2005). Although there is general agreement that DSB repair (DSBR) events are inherently two sided, the extent of resection and/or heteroduplex formed on each side of the DSB is not clear. Petes and colleagues (Porter *et al.* 1993; Merker *et al.* 2003) have suggested two physical models whereby heteroduplex DNA is formed on only one side of the break. Porter *et al.* (1993) suggest that one-sided events might derive from substantial resection of one side of the DSB but not the other, while Merker *et al.* (2003) suggest that the extent of heteroduplex formed upon invasion is short, while that of strand capture is long (Figure 2). Either of these mechanisms leads to extensive heteroduplex formation on only one side of the DSB. The model of Merker *et al.* (2003) is illustrated in Figure 2, A–D. As an alternative mechanism, Foss *et al.* (1999) propose that two-sided events are processed to one-sided events by heteroduplex repair of one of the markers to the parental configuration (also known as restoration; Figure 2, J and K). All of the above experiments require that the interacting DNA strands are identifiable. Therefore, heteroduplex DNA must remain unrepaired (Figure 1). To accomplish this, palindromes have been the preferred genetic markers for these studies. Heteroduplex that contains palindromes is poorly repaired (*i.e.*, fewer 6:2 or 2:6 full conversions), due to the fact that palindromes are partially refractory to mismatch repair by the Msh2p/Mlh1p mismatch repair system (Nag *et al.* 1989). This is presumably due to the failure of mismatch repair proteins to process the palindrome when found in heteroduplex DNA (Alani 1996). The failure to remove the palindrome allows the monitoring of heteroduplex DNA in the end products of the meiotic recombination event (*i.e.*, as 5:3 or 3:5 half conversions/postmeiotic segregation in the tetrads).

The mismatch repair proteins of *Saccharomyces cerevisiae* are orthologs of the *Escherichia coli* long-patch repair proteins MutS and MutL. Heterodimers of Msh2p and either Msh3p or Msh6p recognize insertion/deletion loops as well as base mispairs. Msh2p/Msh3p and Msh2p/Msh6p

[1]*Corresponding author:* Department of Genetics, University Rd., Adrian Bldg., University of Leicester, Leicester LE1 7RH, United Kingdom. E-mail: rhb7@le.ac.uk

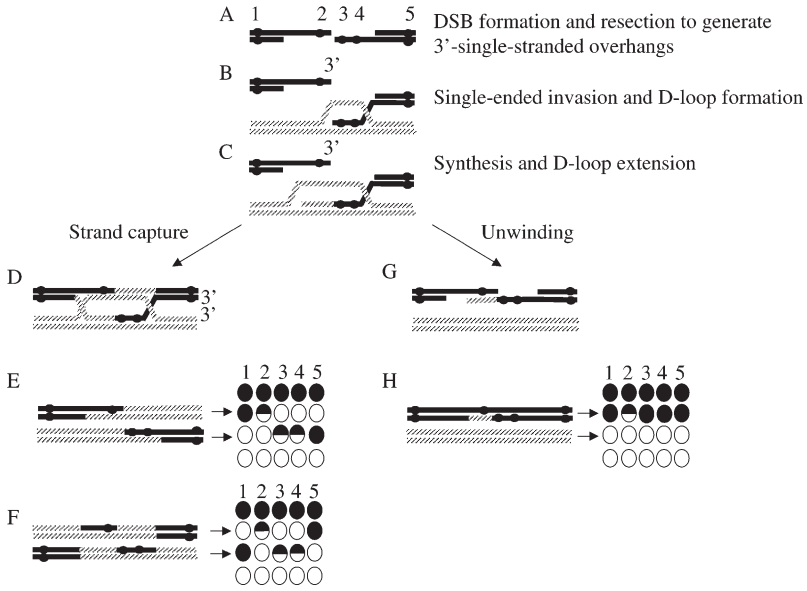

FIGURE 1.—A modified double-strand break repair model and a synthesis-dependent single-strand annealing (SDSA) for recombination. Five markers, labeled 1–5 and spanning the DSB, are shown as solid circles. These correspond to *HPH*, *BIK1-939*, *his4-ATC*, *HIS4-1605*, and *NAT*, as illustrated in Figure 3. Markers 2, 3, and 4 are included in heteroduplex DNA and are left unrepaired so that the origin of the DNA strands is clear. Markers 1 and 5 are flanking markers used to assess crossovers. For simplicity, only the two interacting chromatids are shown. (A) DSB formation and subsequent resection initiates meiotic recombination and generates 3′-single-stranded overhangs. (B) Invasion of the intact homologous chromosome by only one of the 3′-single-stranded overhang generates a D-loop. This is the first stage during which heteroduplex DNA may be formed. Synthesis (C) and subsequent capture of the D-loop by the second end lead to formation of the joint molecule (double Holliday junction; D). Double Holliday junctions may give rise to crossovers (E and F). The resulting tetrads are shown to the right. The spores arising from the interacting DNA molecules are indicated by arrows. The parental chromatids are shown above (all markers solid) and below (all markers open). Markers are as given in A. (G) The D-loop, shown in C, may also be disassembled, leading to SDSA. In the absence of heteroduplex repair, SDSA will generate a one-sided event (marker 2) that will not be associated with a crossover.

heterodimers subsequently form a tetramer with a heterodimer consisting of Mlh1p with Pms1p, Mlh2p, or Mlh3p that is presumed to recruit repair enzymes (reviewed in SURTEES *et al.* 2004). We hypothesized that if the model of Foss *et al.* (1999) was correct, and if restorational repair is dependent on Msh2p and/or Mlh1p, then deleting *MSH2* or *MLH1* should allow all two-sided events to be detected (Figures 1 and 2). On the other hand, if, as is implicit in the Foss *et al.* (1999) model, restorational repair is at least partially independent of conventional mismatch repair, then abolishing mismatch repair should mimic the results obtained with palindromic markers. Furthermore, neither of the models put forth by Petes and colleagues predict an effect of abolishing Msh2p/Mlh1p-dependent mismatch repair. We tested these predictions by deleting *MLH1* or *MSH2* in appropriately marked strains. When selecting tetrads in which one marker had undergone a NMS, we found a decrease in the proportion of two-sided events in the *msh2*Δ and *mlh1*Δ strains compared to wild type. In other words, DSB repair events are initially two sided but are processed to one-sided events in the absence of Msh2p/Mlh1p. We suggest that in the absence of Msh2p and Mlh1p restorational repair can occur and/or that Msh2p and Mlh1p actively promote two-sided events.

MATERIALS AND METHODS

Genetic analysis: Standard genetic procedures and omission media were used as described previously (ABDULLAH and BORTS 2001). The alleles used to study meiotic segregation at the *HIS4* hotspot (*his4-ATC*, *BIK1-939*, and *HIS4-1605*) are described below. The *ade1-1*, *met13-2*, *trp5-1*, *leu2-r*, and *CYH2* alleles have all been described previously (ABDULLAH and BORTS 2001; ABDULLAH *et al.* 2004) as have the *Hph*^{R}*/HYG* and *Nou*^{R}*/NAT* genes (GOLDSTEIN and MCCUSKER 1999).

Double-strand break analysis: Diploid strains were induced to undergo sporulation in liquid as described previously (GOYON and LICHTEN 1993) and samples were collected for DSB analysis at 0 and 24 hr. Genomic DNA was isolated using standard procedures (BORTS *et al.* 1986). Genomic DNA concentrations were determined using the KODAK 2000 Image Station with the KODAK 1D v3.5 software to determine the integrity and concentration of DNA. Plasmid DNA (pEH12) and λ*Bst*EII ladder (New England Biolabs, Beverly, MA) were labeled using the genes images random labeling module (Amersham Pharmacia) following the instructions of the supplier. To visualize the *HIS4* double-strand break hotspot, 1 μg of genomic DNA was digested with *Xba*I (New England Biolabs) and the DNA fragments were separated on a 1.1% agarose gel. DNA was transferred to a solid membrane (SOUTHERN 1975; SAMBROOK *et al.* 1989) and hybridized with labeled probes detected following the manufacturer's instructions (Amersham Pharmacia).

Quantification of DSBs: Chemiluminescence was quantified using a CCD camera (Kodak Image Station 2000; see above). Similar to quantification using radioactivity, chemiluminescence is proportional to the amount of probe hybridized and therefore the amount of homologous DNA on the filter when probe is in excess. The emitted signal was linear with time and with amount of DNA over the experimental ranges utilized (data not shown). Chemiluminescence was also detected by exposure to film. For bands too faint for the camera to detect, film was digitized and quantified. The amount of signal detected on film was also linear with concentration of DNA and time of exposure. The intensity of DSBs was quantified using the KODAK 1D v3.5 software.

Strains: All of the strains were derivatives of *S. cerevisiae* strain Y55 and have been described previously (HOFFMANN *et al.* 2003). All of the mutant strains were isogenic derivatives of EY97 and EY128 (Table 1). The spore viability of the wild-type strains was 95%. ERY102 had a spore viability of 86% and

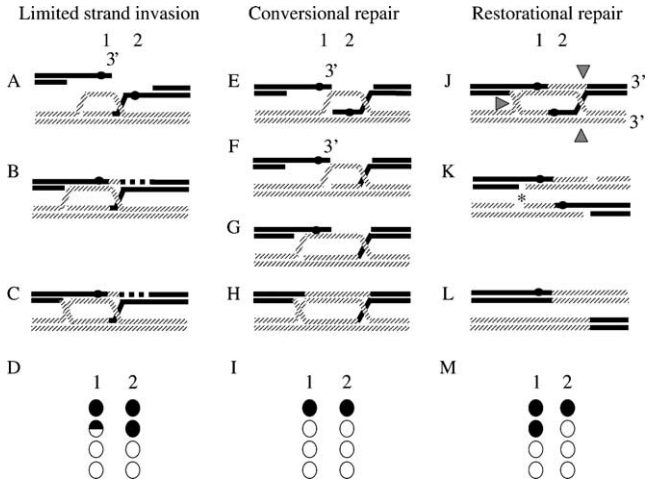

Figure 2.—Models for the origin of sidedness. Markers 1 and 2, corresponding to *BIK1-939* and *his4-ATC*, flank the double-strand break. The tetrads resulting from the DNA interactions are illustrated below, as in Figure 1. Only the two interacting DNA strands are illustrated, but the top and bottom line of the tetrad show the parental configuration of the two uninvolved strands. (A) Limited strand invasion. Invasion of the 3′-single-strand overhang does not include marker 2, shown as a solid circle. D-loop capture by the left-hand side of the DSB (B) and DSB repair synthesis will generate a double Holliday junction (C; redrawn from Merker *et al.* 2003). Marker 2 is not included into heteroduplex DNA at any stage and therefore shows Mendelian segregation (D). When marker 1 remains unrepaired or is converted, a one-sided event results. Conversional repair: The single-end invasion generates heteroduplex DNA containing marker 2 (E). Early mismatch repair of marker 2 (F) leads to a full gene conversion. For marker 1, placed on the left-hand side of the DSB, heteroduplex is formed upon capture of the second end (G). Mismatch repair directed by this end (H) results in this genetic marker undergoing a full conversion as well, thereby generating a two-sided event (I). Nick-directed restorational repair. If early heteroduplex repair is inefficient, as has been suggested for palindromic markers (see text), the heteroduplex DNA persists while the double Holliday junction is formed (J). Cutting of the double Holliday junction to yield a crossover (configuration in Figure 1E), indicated by shaded arrowheads, generates nicks that can be used to direct the mispair removal. If the nicks from only one Holliday junction are used, indicated by an asterisk in K, to direct mispair removal, marker 1 would be restored and marker 2 would be converted (L). Consequently, a one-sided event would result (M). Use of both nicks can lead to both one- and two-sided events (not illustrated).

ERY112 of 83%. The spore viabilities of all of these strains agree with those observed previously (Hoffmann *et al.* 2003).

Plasmids: The *HIS4* (pEH24) and *BIK1* (pEH13) ORFs and the surrounding sequences were PCR amplified from *S. cerevisiae* Y55 using *Pfu* polymerase (Stratagene, La Jolla, CA) and cloned into pMOSBlue (Amersham Pharmacia; Table 2). *KlURA3* was PCR amplified from pWJ716 (Erdeniz *et al.* 1997) and cloned into the *Sma*I site of pEH24 to yield pEH26. Mutations were introduced into *HIS4* and *BIK1* using the quick change site-directed mutagenesis kit (Stratagene, Cambridge, UK) following the manufacturer's instructions. pEH27, containing the *his4-ATC* allele, and pEH28, containing the *HIS4-1605* mutation, were constructed from pEH26 using primer sets *HIS4*.g3c.F plus *HIS4*.g3c.R and *HIS4*.c1605g.F plus *HIS4*.c1605g.R, respectively (Table 3). *HIS4-1605* has a silent guanosine-to-cytosine change that deletes a *Hha*I site. Similarly, *BIK1-939* was created in pEH13 using the *BIK1*.g939a.F and *BIK1*.g939a.R primers, resulting in pEH19. This change results in a silent guanisine-to-adenosine change that deletes a *Pvu*II site in the *BIK1-939* allele.

Construction of alleles: The *his4-ATC* and *BIK1-939* mutant alleles were verified by sequencing around the mutations and introduced into the genome using a cloning-free method described previously (Erdeniz *et al.* 1997). The primers labeled ".adaptermer" in Table 3 were used for this purpose. *HIS4-1605* was introduced by replacing 250 bp to each side of the *Hha*I site with *KANMX4* (primers *HIS4*-1605MX4.F and .R; Table 3). The *KANMX4* cassette was then replaced by transformation with the mutated pEH28 fragment, selecting for histidine prototrophy. All of the introduced alleles were verified by sequencing.

The *HIS4* locus was flanked by the hygromycin B resistance gene (*HPHMX4*, or *HPH*) upstream of *FUS1* (inserted 5130 bp upstream of the start of the *HIS4* ORF, deleting 7 bp), and the nourseothricin resistance gene (*NATMX4*, or *NAT*) was inserted 3804 bp downstream of *HIS4* (the oligonucleotides are listed in Table 3 under "Insertion"). PCR, Southern blotting, and genetic linkage to *HIS4* were used to check both insertions.

Colony PCR: The silent alleles at *BIK1-939* and *HIS4-1605* were analyzed by colony PCR. The entire colony ($\sim 10^7$ cells) was resuspended in 20 μl 0.02 m NaOH. These resuspended colonies can be used for PCR for at least 6 months if stored at 4°. From this, 2 μl was added to a standard PCR reaction (Jeffreys *et al.* 1990) containing either the primer set for *BIK1* or *HIS4* amplification in a total volume of 10 μl. The allele present in the PCR product was determined by restriction digestion with either *Pvu*II or *Hha*I (New England Biolabs), according to the manufacturer's instructions, followed by electrophoresis. Wild-type information at *HIS4-1605* yields two bands of 100 and 400 bp, whereas the mutation at *Hha*I results in a single 500-bp band. Similarly, by destroying the *Pvu*II site in *BIK1-939*, the two wild-type bands of 200 and 600 bp now result in a single 800-bp band. The PCRs yielded results with a range of cells (from <10 to 10^7) and were able to detect the minority band when cells containing the majority information were in 10^4-fold excess (data not shown).

Reconstruction experiment: To determine the probability of detecting a half conversion of either *HIS4-1605* or *BIK1-939*, we performed a reconstruction experiment as follows: Spore colonies mimicking a half-conversion at *BIK1-939*, *his4-ATC*, and *HIS4-1605* were "constructed" by placing a single cell from each parent adjacent to each other on a YEPD plate. For this purpose, it was necessary to change the mating type of one of the parents to prevent the two haploid cells from mating (EY255 was derived from EY97, but expressed the *MAT***a** allele rather than *MAT***a**; Table 1). In total, 83 reconstructed colonies were analyzed, all of which contained half conversions at *his4-ATC* as detected genetically by sectoring for His^+. Segregations of *HIS4-1605* and *BIK1-939* were analyzed by colony PCR as described above. At *HIS4-1605*, all of the 83 reconstructed colonies contained both parental bands in approximately equal proportions. This indicates that the *HIS4-1605* allele does not influence the growth rate compared to the wild-type *HIS4*. Similarly for *BIK1-939*, 82 of the colonies contained all three bands in approximately equal proportions, again suggesting that the single-base change does not influence the growth rate. However, one of the colonies showed only mutant information; hence the failure rate of detecting a half conversion at *BIK1-939* was 1.2% (1/83). On the basis of this experiment we are 95% certain of detecting heteroduplex DNA in ≥95% of the cases encompassing *his4-ATC*, *HIS4-1605*,

TABLE 1

Strains used in this study

Strain	Genotype
Haploids	
EY97	*MAT*α, *LEU2*, *FUS1-HPH*; *his4-ATC*; *RRP7-NAT*; *ade1-1*; *trp5-1*; *cyh2-R*; *lys2-c; ura3-1*
EY128	*BIK1-939*; *HIS4-1605*; *leu2*-r; *met13-2*; *lys2-d*; *ura3-1*
EY111	As EY97 but *msh2*Δ*::KANMX4*
EY129	As EY128 but *msh2*Δ*::KANMX4*
EY130	As EY97 but *mlh1*Δ*::KANMX4*
EY131	As EY128 but *mlh1*Δ*::KANMX4*
EY201	As EY97 but *com1*Δ*::KANMX4*
EY203	As EY128 but *com1*Δ*::KANMX4*
EY255	As EY97 but *MAT***a**
Diploids	
ERY102	EY111 × EY129 (*msh2*Δ*/msh2*Δ)
ERY103	EY97 × EY128
ERY112	EY130 × EY131 (*mlh1*Δ*/mlh1*Δ)
ERY188	EY201 × EY203 (*com1*Δ*/com1*Δ)

and *BIK-939*. These frequencies are similar to those observed previously (Porter *et al.* 1993; Hillers and Stahl 1999).

Statistical analysis: Statistical tests were applied as indicated throughout (Sokal and Rohlf 1995; http://faculty.vassar.edu/lowry/VassarStats.html). $P < 0.05$ was considered significant, except when multiple data sets were analyzed using pairwise comparisons. In such cases, the Dunn-Sidak adjustment of the *P*-value was used (Sokal and Rohlf 1995) to avoid a type I error, as applied previously (Hoffmann *et al.* 2003).

RESULTS

Rationale and terminology: To test predictions regarding the deposition of heteroduplex DNA and crossovers that can made from the models discussed above, we flanked the *HIS4* hotspot with genetic markers. The proportion of events that flanked the DSB (two-sided events) was then determined in wild-type and mismatch-repair-defective strains. According to Merker *et al.* (2003), the absence of mismatch repair proteins should have no effect on the proportion of two-sided events, whereas the model by Foss *et al.* (1999) predicts a decrease in two-sided events in the mismatch-repair-defective strains. Furthermore, the Foss *et al.* (1999) model predicts that crossovers associated with one-sided events should map to a specific interval.

The terminology used to describe tetrads in which more than one genetic marker segregates is as follows: When two markers segregate independently of each other because the heteroduplex DNA that contained them arose from two different DSB repair events, we term this a "co-event." When the two alleles show non-Mendelian segregation consistent with heteroduplex formation and/or repair of a single DSB, the two markers are said to display co-conversion. Conversions could be either full conversions (6:2 or 2:6) or half conversions (5:3 or 3:5, also known as postmeiotic segregations). When reporting ratios of NMS (*e.g.*, 6:2), the genotype of EY128 is given first. This corresponds to wild type for *his4-ATC*, but not for *BIK1-939* and *HIS4-1605*, and to growth on nourseothricin and hygromycin-B-containing medium. DSBR refers to any mechanism that involves strand invasion. Restorational repair refers to removal of a mispair from heteroduplex DNA such that a 4:4 segregation was obtained. Similarly, conversional repair leads to 6:2 or 2:6 segregation. Heteroduplex repair can refer to either. MMR is used only in the context of mismatch removal by Msh2p/Mlh1p. Mispair removal is used when the repair system has not been experimentally established.

***S. cerevisiae* Y55 contains a strong *HIS4* double-strand break hotspot:** Two strains differing in intensity and in the distribution of DSBs within the *HIS4* promoter have been characterized (Fan *et al.* 1995; Baudat and Nicolas 1997; Gerton *et al.* 2000). To demonstrate that the *S. cerevisiae* Y55 strain also contains a *HIS4* DSB hotspot, we analyzed genomic DNA from a strain (ERY188; Table 1) that accumulates unprocessed DSBs (McKee and Kleckner 1997; Prinz *et al.* 1997; see materials and methods). Upon *Xba*I digestion of the genomic DNA

TABLE 2

Plasmids

Plasmid	Description
PMOSBlue (Stratagene)	
pEH12	*HIS4* ORF into pMOSBlue
pEH13	*BIK1* ORF including the upstream 500 and downstream 223 into pMOSBlue
pEH19	pEH13 but change *BIK1-939* g → a (Δ*Pvu*II site)
pEH24	*HIS4* ORF and upstream 1000 bp into pMOSBlue
pEH26	pEH24, but *KlURA3* PCR into *Sma*I site
pEH27	pEH26 but change *HIS4-1605* c → g (Δ*Hha*I site)
pEH28	pEH26 but change *HIS4-3* g → c
pAG25 and pAG32	*HPHMX4* and *NATMX4* plasmids (Goldstein and McCusker 1999)
pRS416	*KANMX4* plasmid (Wach *et al.* 1994)

All plasmids were verified by sequencing the relevant parts of the insertion.

TABLE 3

Oligonucleotides used in this study

Primer	Sequence (5′ → 3′)
Mutagenesis	
HIS4-g3c.F	TTTTTTCTGAATAATCGTTTTGCCGATTCTACCG
HIS4-g3c.R	CGGTAGAATCGGCAAAACGATTATTCAGAAAAAA
HIS4.g3c-adaptamerA.F	AATTCCAGCTGACCACCATGTATGACTATGAACAGTAG
HIS4.g3c-adaptamerB.R	GATCCCCGGGAATTGCCATGACCAACCCTAGACAACGCTC
HIS4.c1605g.F	CCAGCTAGAACAATCTTGGAAGCCCCAACTTTTTCTGCGAC
HIS4.c1605g.R	GTCGCAGAAAAAGTTGGGGCTTCCAAGATTGTTCTAGCTGG
HIS4-1605-MX4.F	TGTCTTGTGTTCCAGATTCCCTCGTCCTATTGAAAAAGTTGGCGTACGCTGCAGGTCGAC
HIS4-1605-MX4.R	CCAAAACTTCACTTGGGCCAGCTGGCATATCAATGGAACATAGAGCATCGATGAATTCGAGCTCG
BIK1.g939a.F	CGAACTCCTGAAAAAACAGCTAGAACAATTACGCAAC
BIK1.g939a.R	GTTGCGTAATTGTTCTAGCTGTTTTTTCAGGAGTTCG
BIK1.g939a-adaptamerA.F	GAACTGACTCTAATAGTGACTCCGGTAAATTAGTTAATTAATTGCGATGATGTAGTTTCTGGTT
BIK1.g939a-adaptamerB.R	ATGTATGTACAACACACATCGGAGGTGAATATAACGTTCCGTGATTCTGGGTAGAAGATCG
Cloning	
HIS4-1000 upstream.F	GAATTACGAGAAGCCCAATTGACCATCGAA
HIS4-ORF.F	ATGGTTTTGCCGATTCTACCGTTAATTGAT
HIS4-ORF.R	CTACTGGAAATCCTTTGGGAACAACCCAAGC
BIK1-500 upstream.F	AGTTGCGTTTGGGAAGAA
BIK1-223 downstream.R	ACAGCGCAGTTGTGCTATGATAT
Insertion	
FUS1-HPH.F	TTGTCATGCACATCATCATACTAAACTTACACGAATAGGAATCGATGAATTCGAGCTCG
FUS1-HPH.R	TTGTCATGCACATCATCATACTAAACTTACACGAATAGGAATCGATGAATTCGAGCTCG
FUS1-A1	CATTGCCGCTTACTCCAAAC
FUS1-A4	CATTGCCGCTTACTCCAAAC
RRP7-NAT.F	TTTAAAGGCATCAATAATTTTTTTCTTTCATATATATTCTGCGTACGCTGCAGGTCGAC
RRP7-NAT.R	TTGTCATGCACATCATCATACTAAACTTACACGAATAGGAATCGATGAATTCGAGCTCG
RRP7-A1	GTGGATGAGGATGGATTCAC
RRP7-A4	CATAACCGACAATCACCGTC
Allele detection	
HIS4.1200-1220.fwd	TCTGTTTTTTTGGAGTACAC
HIS4.1700-1681.rev	GGACCCAAGATCTTATCCAC
BIK1.751-771.fwd	AAGCAACAATTGGAGCTCGAACGC
BIK1.1323-1300.R	CTAGAAGAACTGCTGGTTGTCAGG

Disruption oligonucleotide primers for *MLH1*, *MSH2*, and *COM1* were designed using the immediate 40–45 bp upstream and downstream and linking these to the *KANMX4* primer sequence. Verification primers were designed upstream and downstream as described previously (Wach *et al.* 1994). Sequences are available upon request.

and probing with the *HIS4* ORF, a DSB within the *HIS4* promoter was expected to give rise to an ~2.4- to 2.6-kb fragment (Figure 3B). The fragment size suggested that the *HIS4* DSB hotspot is placed ~300 bp upstream of the *HIS4* start codon. This places *BIK1-939* and *his4-ATC* 350 and ~300 bp, respectively, on opposite sides of the *HIS4* DSB. Quantification indicated that ~4–5% of the total DNA was cut at the *HIS4* hotspot. Other, less strong DSBs were observed at *HPH* (Figure 2B; <0.5%) and *NAT* (data not shown); however, no other DSBs were detected within ~4 kb spanning the *HIS4* DSB.

Deletion of *MSH2* or *MLH1* leads to an increase in non-Mendelian segregation and a decrease in heteroduplex repair: As observed previously, the *msh2*Δ and *mlh1*Δ strains showed an increase in non-Mendelian segregation (Alani *et al.* 1994; Prolla *et al.* 1994). The NMS frequencies of the *his4-ATC*, *HIS4-1605*, *BIK1-939*, *leu2-R1*, *ade1-1*, *trp5-1*, *cyh2*, and *met13-2* alleles were all increased in the *mlh1*Δ strain and at seven of the eight loci in the *msh2*Δ strain (Table 4). The probabilities for such directional increases in aberrant segregation frequencies were 0.0039 and 0.03, respectively (exact binomial probabilities). Such an effect has been observed previously in the absence of functional mismatch repair (Alani *et al.* 1994; Prolla *et al.* 1994; Hunter and Borts 1997; Hoffmann *et al.* 2003). Moreover, heteroduplex intermediates at all of the genetic markers were removed less efficiently (increased half conversions/postmeiotic segregations) in the *mlh1*Δ and *msh2*Δ strains compared to the wild-type strain (Table 5; data not shown).

The total NMS frequency of *his4-ATC* was increased compared to the wild-type strain in both the *mlh1*Δ and

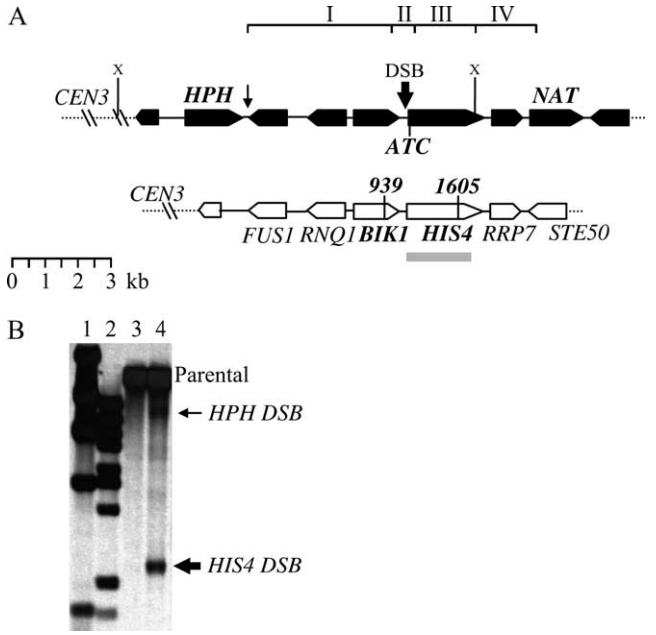

FIGURE 3.—The *HIS4* region on the left arm of chromosome *III* (Crick strand). The chromosome is drawn opposite to the conventional orientation. (A) The two haploid parents EY97 (top chromatid; solid) and EY128 (bottom chromatid; open) are shown. The direction of transcription is indicated by the tapered end. The boxes labeled *NAT* and *HPH* represent insertions introduced in EY97 but not in EY128. EY97 is auxotrophic for histidine synthesis as the start codon of *HIS4* has been changed from ATG to ATC (*his4-ATC* allele). *HIS4* and *BIK1* of parent EY128 contain silent single nucleotide changes at *HIS4-1605* and *BIK1-939*. The regions between *HPH* and *BIK1-939*, *BIK1-939* and *his4-ATC*, *his4-ATC* and *HIS4-1605*, and *HIS4-1605* and *NAT* to which crossovers could be mapped are labeled interval I, II, III, and IV, respectively. (B) Mapping of DSBs within the *HIS4* region. Lanes 1 and 2 contain the size standards λ*Hin*dIII and λ*Bst*EII, respectively. Meiotic time course DNA from strain ERY188 was extracted after 0 hr in sporulation medium (lane 3) or after 24 hr (lane 4). The DNA was digested with *Xba*I indicated by an "X" in A and the Southern blot was probed with the *HIS4* ORF (shaded bar in A). Arrows to the right indicate the position and relative intensities of the two DSBs in the region.

*msh2*Δ strains (compare 14% to 20% and 18%, respectively; Table 5). The frequencies of NMS of *BIK1-939* were less than that of *his4-ATC* (9.3, 13, and 8.9% in the wild-type, *mlh1*Δ, and *msh2*Δ strains, respectively; Table 5) in all of the three strains. This may be because *BIK1-939* is placed ~50 bp farther from the *HIS4* DSB and is less likely to be included in heteroduplex DNA or because *BIK1-939* mispairs are more readily restored compared to *his4-ATC* mispairs in all three strains. Finally, the repair of heteroduplex DNA containing either allele was decreased in the mismatch repair mutants. The repair rate containing *BIK1-939* was decreased from 100% to 0% in the *mlh1*Δ strain and to 21% in the *msh2*Δ strain (Table 5; *mlh1*Δ subset and *msh2*Δ subset). The repair rate of *his4-ATC* was decreased from 87% in the wild-type strain to 12% and 37% in the *mlh1*Δ and *msh2*Δ strains, respectively. The repair rate of *his4-ATC* in the *msh2*Δ strain was higher than that in the *mlh1*Δ strain ($P < 0.05$; *z*-test for proportions). The NMS frequencies and heteroduplex repair of the *NAT* and *HPH* markers were not affected in the *mlh1*Δ and *msh2*Δ strains. Since it is known that the removal of large insertion/deletions such as *NAT* and *HPH* present in meiotic heteroduplex DNA is independent of the mismatch repair system (KEARNEY *et al.* 2001), *NAT* and *HPH* were excluded from the analysis above.

The proportions of co-events and co-conversions were decreased in *mlh1*Δ and *msh2*Δ strains: Tetrads in which *his4-ATC* showed a NMS were identified ("selected" in Table 5) and analyzed for NMS at *BIK1-939* and *HIS4-1605* (the marker configurations of all these tetrads are illustrated in the supplementary appendix at http://www.genetics.org/supplemental/). In the wild-type strain, 144 of the 243 tetrads showing NMS at *his4-ATC* were analyzed. In the wild-type strain, 69% of events were co-events of *his4-ATC* and *BIK1-939*, whereas in the *mlh1*Δ and *msh2*Δ strains there were significantly fewer (44% and 45%, respectively; $P < 0.025$; *z*-test for proportions).

Identification and analysis of complex events: Co-events may not be an accurate measure of two sidedness as "complex events," consisting of more than one DSB repair event, may obscure the actual proportion of two-sided events. Tetrads that contained more than two recombinant chromatids in the *HIS4* interval (Figure 4; supplementary material section 1A at http://www.genetics.org/supplemental/) most likely arose from multiple initiations. Finally, tetrads that contained two recombinant spores in which the NMS of *BIK-939* and *his4-ATC* had arisen from repair of more than a single DSB were also considered complex (supplementary material section 1B at http://www.genetics.org/supplemental/; Figure 4D). All three strains contained a similar proportion of such complex events. This resulted in 38%, 30%, and 36% of the tetrads that showed non-Mendelian segregation for *his4-ATC* being excluded from further analysis in the wild-type, *mlh1*Δ, and *msh2*Δ strains, respectively (Table 6; supplementary material section 1A at http://www.genetics.org/supplemental/). These values are similar to those observed previously at *HIS4* (HILLERS and STAHL 1999; MERKER *et al.* 2003). The majority of these complex events (>70%) can be explained in terms of two independent DSB repair events initiated from the *HIS4* promoter. This is consistent with no other DSBs having been detected within the *HIS4* region.

It was possible that the wild-type strain only appeared to contain more two-sided events compared to the mutant strains. This would be the case if a greater proportion of two-sided events in the mutants were complex events and therefore excluded from the analysis. In the wild type, approximately two-thirds of the complex events were two sided. Since the proportions of two-sided complex events in the *mlh1*Δ and *msh2*Δ strains were similar (Table 6), we conclude that eliminating complex events

TABLE 4

Non-Mendelian segregation of several loci

	Allele							
Strain	*his4-ATC*	*HIS4-1605*[a]	*BIK1-939*[a]	*leu2-R1*	*ade1-1*	*met13-2*	*cyh2*	*trp5-1*
Wild-type	14 (243/1731)	2.8 (8/289)	9.3 (10/107)	1.7 (29/1731)	2.0 (36/1731)	4.5 (78/1731)	0.6 (11/1731)	0.9 (16/1731)
*mlh1*Δ	20[b] (116/585)	5.6 (6/106)	13 (14/106)	2.7 (16/585)	3.6 (21/585)	5.5 (32/585)	1.4 (8/585)	1.4 (8/585)
*msh2*Δ	18 (96/545)	4.0 (4/101)	8.9 (9/101)	2.2 (12/545)	2.8 (15/545)	2.6 (14/545)	0.9 (5/545)	2.9 (16/545)

NMS is given as the percentage of total half-conversion and full-conversion events divided by the total number of tetrads analyzed. The actual number of tetrads with an NMS event and the total number of tetrads are given in parentheses.

[a] Randomly selected tetrads were analyzed for the wild-type, *mlh1*Δ, and *msh2*Δ strains to estimate the overall frequency of NMS at *HIS4-1605* and *BIK1-939*.

[b] Values significantly different from the wild-type strain using a *G*-test. *P*-values <0.05 were considered significant. None of the values from the subsets were different from the corresponding main data set (*G*-test). Therefore, the subsets are representative of the main data sets.

could not account for the decreased proportion of two-sided events in the *mlh1*Δ and *msh2*Δ strains.

Identification of true co-conversion events: To identify true co-conversions, and thus two-sided events arising from a single DSB repair event, only tetrads in which no more than two spores were recombinant were analyzed. These tetrads were placed into the classes given in Table 6. Tetrads in which *his4-ATC*, but not *BIK1-939*, showed NMS were considered to be one-sided events. When *his4-ATC* and *BIK1-939* segregated in a fashion predicted by the DSBR model (Figures 1 and 4), the DSBR event was considered two sided. If other markers showed a co-event, the DSBR event was considered potentially two sided. Similarly, when *his4-ATC* and *BIK1-939* showed a co-event not predicted by the DSBR models, the co-event was considered two sided but not due to a single DSBR event. Using only the co-conversions to estimate the proportion of two-sided events, 63% of the events in the wild-type strain were two sided. In contrast, only 31% of events were two sided in the *mlh1*Δ and 28% were two sided in the *msh2*Δ strains ($P < 0.025$; *z*-test for proportions; Table 6). Thus, the decrease in the proportion of co-events in the two mutant strains was also reflected in the decrease in two-sided co-conversion events arising from a single DSB repair event.

Potential sources of error: One reason for the apparent decrease in the proportion of co-conversions in the mutant strains may be the erroneous classification of events as two sided in the wild-type strain, since the wild type contained very few informative tetrads (half conversions at *BIK1-939* as well as at *his4-ATC*). For example, the apparent two-sided events might have been the result of two independent DSB repair events that by chance looked like a co-conversion. However, from the number of events that unambiguously arose from multiple initiations (two-strand complex, Figure 4D and Table 6), we estimated the number of co-conversions of *BIK1-939* and *his4-ATC* that were the consequence of two different meiotic DSBs and arose by chance. If two non-Mendelian segregation events arose from two independent DSB repair events, then a 6:2 (6 white strands:2 black strands) non-Mendelian segregation of *his4-ATC* should be equally likely to be associated with a 6:2 or a 2:6 non-Mendelian segregation of *BIK1-939* (Figure 4, C or D). For example, tetrads in which *his4-ATC* shows a 6:2 NMS while *BIK1-939* shows a 2:6 NMS (Figure 4D) can have come only from two initiations. Therefore, a number of *his4-ATC* and *BIK1-939* co-conversions, where both markers converted in the same direction, for example, 6:2/6:2's (Figure 4C), could have arisen from two independent initiations. This number of apparent co-conversions is equivalent to the number of obvious co-events (Figure 4D). Since the wild-type strain had four such events, the 57 co-conversion events (Table 6) contained an equivalent number of co-events that were in the correct pattern by chance (and thus would mimic co-conversion events). Therefore, we estimated that only 53 of the 57 co-conversions were real co-conversions. This is still a significantly greater proportion than that predicted by chance ($P < 0.05$, χ^2 goodness-of-fit test). In addition, the wild-type adjusted co-conversion frequency was significantly greater than that of the Mlh1p- and Msh2p-deficient mutant strains (compare 53/90 to 25/81 and to 17/61; $P < 0.025$, *z*-test for proportions; pairwise comparisons). The values for the mutant strains were not adjusted since their adjustment would only exacerbate the differences between wild type and mutants.

G-G mismatches are restored in the *mlh1*Δ and *msh2*Δ strains: Since DSBs occur with equal frequency on both parental strands (data not shown), the frequency of 5:3/6:2 non-Mendelian segregations should equal the frequency of 3:5/2:6 non-Mendelian segregations, as was observed in the wild-type strain. However, in the *mlh1*Δ and *msh2*Δ strains there was a deficit of 5:3 half conversions compared to 3:5 half conversions at *his4-*

TABLE 5

Non-Mendelian segregation of *his4-ATC* and *BIK1-939*

Allele	Relevant genotype	NMS class										Total NMS	Total tetrads	NMS (%)	FC/NMS (%)
		6:2	2:6	5:3	3:5	8:0	0:8	7:1	1:7	Ab4:4	Others[a]				
his4-ATC	Wild type	96	111	14	15	1	3	1	2	0	0	243	1731	14	87
	*mlh1*Δ	5	7	35	65	0	0	0	0	2	2	116	585	20[b]	12
	*msh2*Δ	15	18	17	36	0	1	0	1	3	3	96	545	18	37
	Wild-type subset[c]	1	7	1	1	0	0	0	0	0	0	10	107	9.3	80
	*mlh1*Δ subset[c]	2	0	9	11	0	0	0	0	0	0	22	106	21	9
	*msh2*Δ subset[c]	2	3	3	11	0	0	0	0	1	1	21	101	21	24
BIK1-939	Wild-type subset[c]	0	9	0	0	1	0	0	0	0	0	10	107	9.3	100
	*mlh1*Δ subset[c]	0	1	6	4	0	2	0	0	1	0	14	106	13	21
	*msh2*Δ subset[c]	0	0	3	6	0	0	0	0	0	0	9	101	8.9	0
	Wild type selected[d]	38	51	2	1	1	6	0	1	0	0	100	144	69	96
	*mlh1*Δ selected[d]	0	3	23	25	1	0	0	0	2	1	51	116	44[b]	10
	*msh2*Δ selected[d]	0	4	14	23	0	0	0	0	2	0	43	96	45[b]	10

FC, full conversion.

[a] Mainly Ab6:2 and Ab2:6.

[b] Statistically significant compared to the equivalent wild-type proportion ($P < 0.025$; *G*-test for homogeneity).

[c] Randomly chosen tetrads were analyzed by PCR to estimate the NMS frequencies of *BIK1-939* and *HIS4-1605*.

[d] Tetrads that were selected for an NMS at *his4*-ATC and were analyzed further for NMS at *BIK1-939* and *HIS4-1605*.

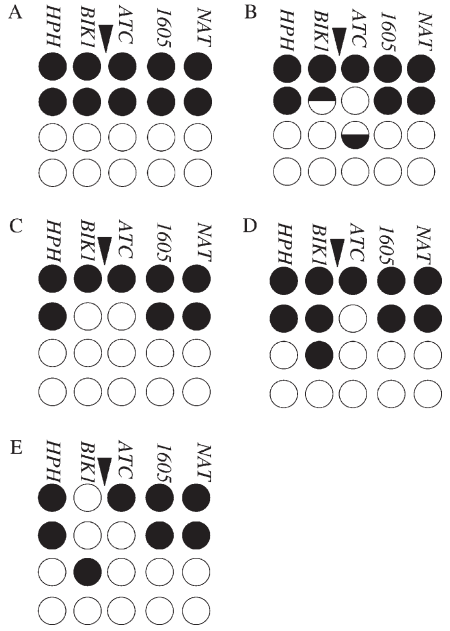

Figure 4.—Co-conversion and co-event tetrads. A tetrad with the parental configuration of the genetic markers is given in A. Each tetrad is shown by four rows and five columns. Each row represents one chromatid and each column represents one marker [*HPH*, *BIK1-939* (*BIK1*), *his4-ATC* (*ATC*), *HIS4-1605* (*1605*), and *NAT*)]. The position of the *HIS4* DSB is indicated by an arrowhead. Open circles signify the EY128 parental information (Figure 3), and solid circles show EY97 parental information (Figure 3). A NMS event is represented as the number of white to the number of black strands. (B) The tetrad illustrated represents a co-half conversion of *BIK1-939* and *his4-ATC*. Such tetrads may arise from unrepaired heteroduplex DNA from a single DSB repair event. The half conversions are placed on two different recombinant chromatids as predicted by the DSB repair model (Figure 1, E and F). The half-conversions occur in the 5:3 and 5:3 orientation for *BIK1-939* and *his4-ATC* as expected for a co-half conversion of markers on opposite sides of the same DSB. (C) Represents *bona fide* full co-conversion events arising from the removal of both mispairs within the heteroduplex DNA from a single DSB repair event as illustrated in Figure 2 (E–I). Other *bona fide* co-conversions arising from the heteroduplex repair of B could have a half conversion at *BIK1-939* accompanied by a full conversion at *his4-ATC* or vice versa (for example, see class 5a and class 677a in the supplementary appendix at http://www.genetics.org/supplemental/). (D) A co-event where the non-Mendelian segregation of the two markers (2:6 and 6:2) is most likely caused by two independent DSB repair events. Mispair removal of the heteroduplex in B cannot account for this type of tetrad. An example of a tetrad that contained three recombinant chromatids is shown in E. Such tetrads, as well as those that contained four recombinant chromatids, were deemed to have arisen from multiple DSB repair events and were excluded from further analysis. Classifications of all tetrads analyzed (supplementary appendix) are given in the supplementary tables at http://www.genetics.org/supplemental/.

ATC that were not compensated for by an increase in 6:2 full conversions (compare 35 to 65 and 17 to 36 in the *mlh1*Δ and *msh2*Δ strain, respectively, Table 5; $P < 0.05$, χ^2 goodness-of-fit test, for both strains). This deficit of 5:3 half conversions suggested that G-G mismatches were restored in the *mlh1*Δ and *msh2*Δ strains. Assuming that we recovered all C-C mispairs as either 2:6 or 3:5's, then the total number of G-G mismatches formed (number of 5:3 + number of 6:2) should equal the total number of C-C mismatches formed (number of 3:5 + number of 2:6). From this we can estimate the rate of restoration of G-G pairs by dividing the number of "missing" G-G mismatches by the total number of G-G mismatches, estimated from the rate of C-C mismatches. In the *mlh1*Δ strain there were 40 observed G-G mismatches (35 tetrads in which *his4-ATC* segregated 5:3 and 5 in which they segregated 6:2; Table 5). Similarly, there were 72 C-C mismatches formed (65 and 7 tetrads, respectively, in which *his4-ATC* segregated 3:5 and 2:6). Thus, 32 G-G mismatches were missing, resulting in a restoration rate of 44% (32/72). Similarly, 41% of the G-G mismatches were potentially restored in the *msh2*Δ strain. Alternatively, if there is some restoration of C-C mispairs in the mutants, then the restoration rates of G-G are underestimated. It is impossible to determine whether C-C mispairs were restored from the genetic data. However, the apparent restoration of G-G mispairs raises the possibility that some of the two-sided events may have been processed to one-sided events in an Msh2p/Mlh1p-independent fashion (see discussion). A similar disparity has also been observed when other poorly repaired markers, such as palindromes, are used (Porter *et al.* 1993; Gilbertson and Stahl 1996; Merker *et al.* 2003; Jessop *et al.* 2005).

Deletion of *MLH1* affects crossing over: Tetrads containing two-sided or one-sided events were analyzed for crossing over (Table 7; see supplementary material at http://www.genetics.org/supplemental/, section 3, for classes included). If the crossover was not immediately adjacent to the genetic marker that showed an aberrant segregation, it was deemed incidental and excluded from the analysis (Merker *et al.* 2003). The map distance in the *mlh1*Δ strain was decreased compared to the wild type. This is in agreement with previous observations that *mlh1*Δ shows decreased crossing over (Hunter and Borts 1997). To ask whether *mlh1*Δ affects the frequency of crossing over associated with one- and/or two-sided events, we divided the events into four classes: one-sided events associated with crossovers, one-sided events associated with noncrossovers, two-sided events associated with crossovers, and two-sided associated with noncrossovers (Table 7). Both MMR mutant strains showed a difference in the distribution of events into those four classes compared to the wild-type strain ($P < 0.05$; *G*-test of homogeneity), reflecting that the *mlh1*Δ and *msh2*Δ strains contain more one-sided events. When we compared the distribution of *mlh1*Δ to that of the *msh2*Δ strain, we did not observe a significant difference. However, given the size of the data sets presented here, we may not have been able to detect any differences.

TABLE 6

One- and two-sided events at the *HIS4* recombination hotspot

Strain	Total *ATC*[a]	Complex[b]			Single events[f]		
		One sided[c]	Two sided[d]	Two DSBR[e]	One sided	Two sided[g]	Potential[h]
Wild-type	144	28 (15/54)	65 (35/54)	7.0 (4/54)	32 (29/90)	63 (57/90)	4.4 (4/90)
*mlh1*Δ/*mlh1*Δ	116	26 (9/35)	46 (16/35)	28 (10/35)	64[i] (52/81)	31[i] (25/81)	4.9 (4/81)
*msh2*Δ/*msh2*Δ	96	34 (12/35)	60 (21/35)	5.7 (2/35)	67[i] (41/61)	28[i] (17/61)	4.9 (3/61)

[a] The total number of NMS events at *his4-ATC* (abbreviated *ATC*) that were analyzed for NMS of *BIK1*-939.
[b] Tetrads in which more than two spores were recombinant for the five genetic markers (*e.g.*, Figure 4E).
[c] The proportion of complex events in which *his4-ATC* but not *BIK1*-939 showed NMS.
[d] The proportion of complex events in which both *his4-ATC* and *BIK1*-939 showed NMS.
[e] Tetrads in which only two spores were recombinant and in which both *his4-ATC* and *BIK1-939* showed NMS but not explicable as coming from a single DSB repair event (Figure 4D).
[f] Tetrads in which no more than two spores were recombinant for the five genetic markers.
[g] The proportion of single events in which both *his4-ATC* and *BIK1*-939 showed co-conversion (two-sided events).
[h] Two-sided events in which both *his4-ATC* and *BIK1*-939 showed NMS according to the DSBR model, although, one additional marker also showed NMS.
[i] Statistically significantly different from the wild-type strain ($P < 0.025$, *z*-test for proportions).

Crossovers map to either side of the non-Mendelian segregation: Foss *et al.* (1999) suggest that two-sided events are processed to a one-sided event (for example, an apparently simple NMS of *his4-ATC*) due to restoration using the nicks generated from Holliday junction cleavage (Figure 2, J–L). If this is correct, then crossovers associated with the apparent one-sided event should map between *his4-ATC* and *BIK1*-939 (interval II). As a test of the model, we analyzed the position of the crossovers associated with one-sided events. Of the 19 informative one-sided events in the two mutant strains, seven crossovers appeared to be incidental, mapping in either interval I or IV (supplementary Table 2 at http://www.genetics.org/supplemental/). Of the remaining crossovers, three mapped to interval II whereas nine mapped to interval III (between *his4-ATC* and *HIS4-1605*). Thus, the crossovers associated with one-sided events did not show a significant bias toward mapping in interval II. We conclude that the one-sided events associated with crossovers do not arise from Holliday junction resolution that was associated with restoration of *BIK1*-939.

Gene conversion tracts are short: Previous studies at *HIS4* have found evidence for long gene conversion tracts and break-induced replication (Merker *et al.* 2003 and references therein). To investigate whether this was also the case in this system, we analyzed co-events between *HPH* and *BIK1-939* as well as *NAT* and *HIS4-1605*. In both cases, co-events were rare. Of all of the unselected tetrads analyzed in the three strains, only 2 tetrads of 314 showed co-events of *BIK1-939* with *HPH*. In these

TABLE 7

Distribution of crossovers and noncrossovers associated with NMS of *his4-ATC*

	% two sided		% one sided		Total events	CO[a]
	CO	NCO	CO	NCO		
Wild type	49 (35)	27 (19)	13 (9)	11 (8)	71	0.68
*mlh1*Δ/*mlh1*Δ[b]	24 (15)	14 (9)	16 (10)	46 (29)	63	0.40[c]
*msh2*Δ/*msh2*Δ[b]	19 (9)	13 (6)	36 (17)	32 (15)	47	0.55

Events were classified as two sided with a crossover, two sided with a noncrossover, one sided with a crossover, or one sided with a noncrossover (for classification see supplementary section 3 at http://www.genetics.org/supplemental/). Incidental crossovers (supplementary Table 2 at http://www.genetics.org/supplemental/) were not included in this analysis. Events in which *HPH* or *NAT* co-converted were excluded as the crossover could not be mapped. CO, crossovers; NCO, noncrossovers.
[a] Calculated as the number of two- and one-sided events associated with a crossover divided by the number of total events.
[b] Distribution of events significantly different from the distribution of the wild-type strain ($P < 0.025$; *G*-test for homogeneity).
[c] Frequency significantly decreased compared to the wild-type strain ($P < 0.025$; *z*-test for proportions).

2 tetrads, *NAT* and *HIS4-1605* also were co-events. Moreover, all of these segregations were 8:0 and thus clearly identifiable as multiple events. Therefore, we did not observe any co-conversions involving *HPH-BIK1-939* and *NAT-HIS4-1605*. Hence, we did not observe any evidence of break-induced replication or very long gene conversion tracts. We also assessed the frequency of co-events between *his4-ATC* and *HIS4-1605*. Fewer than 10% of tracts extended as far as *HIS4-1605* (1.6 kb from *his4-ATC* and ~1.9 kb from the DSB). Thus, most gene conversion tracts at *HIS4* were short.

DISCUSSION

***MSH2* and *MLH1* mutants have fewer two-sided events:** The loss of Msh2p/Mlh1p-mediated mismatch repair could have one of three possible outcomes, depending on its role(s) in recombinational DNA transactions. First, the proportion of two-sided events could be increased, as all heteroduplex DNA would be recovered (Figures 1 and 2) due to the absence of any mispair removal. Second, if the extent of 3′-tail invasion/assimilation were the sole determinant of sidedness, then deletion of Msh2p/Mlh1p should have no effect (Figure 2, A–D). Third, the proportion of two-sided events would be decreased if Msh2p/Mlh1p-directed mispair removal from the invading/captured strand's end "fixed" heteroduplex DNA as full conversions and in its absence they became subject to restorational repair (Figure 2, E–H). Finally, a similar decrease in two-sided events is expected if mismatch repair proteins actively promote two-sided events. In the absence of Msh2p/Mlh2p, we found that the proportion of two-sided events was significantly decreased, indicating that the latter possibilities are more likely.

Models for Msh2p/Mlh1p functions: We can envision a number of mechanisms by which Msh2p/Mlh1p might promote two-sided events. In the first, Mlh1p and Msh2p modulate strand invasion such that a greater proportion of the 3′-tail invades the homolog and/or a greater proportion of heteroduplex DNA is formed upon strand capture. The Mer3p helicase has recently been demonstrated to carry out strand assimilation (Mazina *et al.* 2004) and has been proposed to promote crossovers. If Msh2p/M1h1p were to facilitate this function, one-sided events might be extended into two-sided events. However, this mechanism is inconsistent with previous proposals for the influence of mismatch repair proteins on heteroduplex formation (reviewed in Borts *et al.* 2000) as well as the lack of a crossover defect in *msh2*Δ strains. It is also inconsistent with the *in vitro* experiments demonstrating that the MutL/S complex disrupts RecA-mediated filament formation in the presence of mismatches (Worth *et al.* 1994, 1998).

A mechanism more consistent with the known activities of mismatch repair proteins is one in which Msh2p/Mlh1p promote two-sided events via mismatch removal from the invading strand by excision. This could lead to destabilization of the strand invasion structure. Such an event might necessitate that the other side of the DSB invades and more extensive heteroduplex DNA than normal is formed. In a wild-type strain, this will always lead to full conversion of any markers involved. In addition, when multiple mismatches are contained in the same heteroduplex, as might occur during SDSA, a second round of recombination extending the conversion tract might occur (Borts and Haber 1987). As these processes are dependent on mismatch repair proteins (Borts *et al.* 1990, 2000), the absence of Msh2p/Mlh1p would cause the proportion of two-sided events to be decreased. No physical evidence addresses these issues.

Foss *et al.* (1999) proposed that markers remaining in heteroduplex until resolution are subject to restoration. This implies a hierarchical removal of mispairs within heteroduplex DNA. During 3′-tail invasion and/or annealing, mispairs are removed using the invading end to direct the removal of the mispair, thus fixing the event as a conversion. When MMR is efficient, a two-sided event can occur (Figure 2, E–I). In contrast, should early removal of the mispair fail—for example, if MMR is absent or inactive—the ends generated from double Holliday junction resolution (Figure 2, J–L) or SDSA (Figure 1G) can be used to direct removal of the mispair. This "late" mispair removal, however, is likely to cause both restorations and conversions due to the positions of the ends. This model, based on data generated using poorly removed palindromes as genetic markers, requires that early and late mispair removal have different properties. Most importantly, the "early" mispair removal must be less able to recognize/remove a palindrome-containing mispair such that it is not converted. The late mispair removal must then be able to remove the palindrome such that restoration or conversion occurs. Both restorational and conversional mispair removal in the absence of Msh2p have been observed (Coic *et al.* 2000), and the data presented here provide additional, albeit indirect, evidence for restorational mispair removal.

The model of Foss *et al.* (1999) also predicts that for one-sided events associated with crossovers, the crossover should be positioned between *his4-ATC* and *BIK1-939* for the nicks generated by Holliday junction resolution to have promoted a restoration of the *BIK1-939* marker. This was clearly not the case. Thus, while the model by Foss *et al.* (1999) is formally possible, we suggest a model that involves restorational repair without assuming that nicks generated from Holliday junction resolution direct mispair removal. In addition, we suggest that Msh2p/Mlh1p-dependent repair is nick directed and is active both during strand invasion/assimilation (early) and after Holliday junction resolution (late: Figure 1, E and F, and Figure 2, J and K) and D-loop disassembly during SDSA (Figure 1G). This would lead

predominantly to full conversions but also some restorations, depending on which late nicks are used to direct mispair removal (*e.g.*, Figure 2, J–L). If SDSA prevails, some of the one-sided events may also be restored, thus leaving no sign of a DSB repair event. In the absence of the Msh2p/Mlh1p nick-directed repair pathway, a less efficient repair pathway may be able to remove some, but not all, of the mispairs in the heteroduplex DNA. However, rather than using nicks, this repair complex may create short, discontinuous heteroduplex repair tracts with no strand bias, as have been observed previously in *msh2*Δ (Coic *et al.* 2000). Without strand bias, there would be a 50% chance of a restoration. This is in good agreement with the observation that the *mlh1*Δ and *msh2*Δ strains contained approximately half the number of two-sided events compared to the wild-type strain (Table 6). This also agrees with the estimate that ~40% of the G-G mispairs are restored.

Palindromes and mismatch repair mutants: The proportion of two-sided events differs markedly between wild-type strains utilizing poorly repaired palindromes (Porter *et al.* 1993; Gilbertson and Stahl 1996; Jessop *et al.* 2005) and those using single-base mismatches as markers for heteroduplex formation (this study and Schultes and Szostak 1990). However, the proportion of two-sided events obtained in the *mlh1*Δ and *msh2*Δ strains with single-base-pair markers was similar to that obtained in wild-type strains using palindromes. There may be several explanations for this. First, palindromes and single nucleotide polymorphisms may have different effects on heteroduplex DNA formation. For example, palindromes may be less likely to be included in heteroduplex DNA. Thus, palindromes may cause events to be one-sided by limiting strand invasion. However, no experimental data have addressed this question. On the other hand, assuming that palindromes are indeed incorporated into heteroduplex DNA as frequently as single nucleotide mispairs, the heteroduplex repair of single nucleotide mispairs in *MLH1* and *MSH2* mutants may be analogous to the failure to remove palindromes in wild-type cells. If this were true, one would predict that for base-pair mismatches, the absence of Mlh1p/Msh2p should mimic the effect of palindromes and therefore have a greater proportion of one-sided events. This is indeed the case (Table 6). Whether palindromes are less frequently incorporated into heteroduplex DNA or subject to alternative repair remains to be determined.

In conclusion, we suggest that in wild-type cells the initial DSB repair event is two sided. The absence of MMR, by either mutation or use of poorly repaired palindromes, allows a second, unbiased mispair removal pathway to restore a proportion of heteroduplex, leading to apparent one-sided events. This is consistent with the observed disparity in the recovery of conversions of palindromes.

We thank Craig Griffin, Jette Foss, Frank Stahl, Michael Lichten, Lea Jessop, Victoria Cotton, and Ed Loius for critical reading of various manuscripts. We thank Jette Foss, Frank Stahl, Lea Jessop, Tom Petes, Ian Hickson, and the anonymous reviewers for helpful comments and discussions. This work was supported by the Wellcome Trust.

LITERATURE CITED

Abdullah, M. F., and R. H. Borts, 2001 Meiotic recombination frequencies are affected by nutritional states in *Saccharomyces cerevisiae*. Proc. Natl. Acad. Sci. USA **98:** 14524–14529.

Abdullah, M. F., E. R. Hoffmann, V. E. Cotton and R. H. Borts, 2004 A role for the *MutL* homologue *MLH2* in controlling heteroduplex formation and in regulating between two different crossover pathways in budding yeast. Cytogenet. Genome Res. **107:** 180–190.

Alani, E., 1996 The *Saccharomyces cerevisiae* Msh2 and Msh6 proteins form a complex that specifically binds to duplex oligonucleotides containing mismatched DNA base pairs. Mol. Cell. Biol. **16:** 5604–5615.

Alani, A., R. A. Reenan and R. D. Kolodner, 1994 Interaction between mismatch repair and genetic recombination in *Saccharomyces cerevisiae*. Genetics **137:** 19–39.

Baudat, F., and A. Nicolas, 1997 Clustering of meiotic double-strand breaks on yeast chromosome *III*. Proc. Natl. Acad. Sci. USA **94:** 5213–5218.

Borts, R. H., and J. E. Haber, 1987 Meiotic recombination in yeast: alteration by multiple heterozygosities. Science **237:** 1459–1463.

Borts, R. H., M. Lichten and J. E. Haber, 1986 Analysis of meiosis-defective mutations in yeast by physical monitoring of recombination. Genetics **113:** 551–567.

Borts, R. H., W.-Y. Leung, K. Kramer, B. Kramer, M. S. Williamson *et al.*, 1990 Mismatch repair-induced meiotic recombination requires the *PMS1* gene product. Genetics **124:** 573–584.

Borts, R. H., S. R. Chambers and M. F. F. Abdullah, 2000 The many faces of mismatch repair in meiosis. Mutat. Res. **451:** 129–150.

Coic, E., L. Gluck and F. Fabre, 2000 Evidence for short-patch mismatch repair in *Saccharomyces cerevisiae*. EMBO J. **19:** 3408–3417.

Erdeniz, N., U. H. Mortensen and R. Rothstein, 1997 Cloning-free PCR-based allele replacement methods. Genome Res. **7:** 1174–1183.

Fan, Q., F. Xu and T. D. Petes, 1995 Meiosis-specific double-strand breaks at the *HIS4* recombination hotspot in the yeast *Saccharomyces cerevisiae*: control in *cis* and *trans*. Mol. Cell. Biol. **15:** 1679–1688.

Foss, G. M., K. J. Hillers and F. W. Stahl, 1999 The conversion gradient at *HIS4* of *Saccharomyces cerevisiae*. II. A role for mismatch repair directed by biased resolution of the recombinational intermediate. Genetics **153:** 573–583.

Gerton, J. L., J. DeRisi, R. Shroff, M. Lichten, P. O. Brown *et al.*, 2000 Global mapping of meiotic recombination hotspots and coldspots in the yeast *Saccharomyces cerevisiae*. Proc. Natl. Acad. Sci. USA **97:** 11383–11390.

Gilbertson, L. A., and F. W. Stahl, 1996 A test of the double-strand break model for meiotic recombination in *Saccharomyces cerevisiae*. Genetics **144:** 27–41.

Goldstein, A. L., and J. H. McCusker, 1999 Three new dominant drug resistance cassettes for gene disruption in *Saccharomyces cerevisiae*. Yeast **15:** 1541–1553.

Goyon, C., and M. Lichten, 1993 Timing of molecular events in meiosis in *Saccharomyces cerevisiae*: stable heteroduplex is formed late in meiotic prophase. Mol. Cell. Biol. **13:** 373–382.

Hillers, K. J., and F. W. Stahl, 1999 The conversion gradient at *HIS4* of *Saccharomyces cerevisiae*. I. Rejection and restoration of Mendelian segregation. Genetics **153:** 555–572.

Hoffmann, E. R., P. V. Shcherbakova, T. A. Kunkel and R. H. Borts, 2003 *MLH1* mutations differentially affect meiotic functions in *Saccharomyces cerevisiae*. Genetics **163:** 515–526.

Hunter, N., and R. H. Borts, 1997 Mlh1p is unique among mismatch repair proteins in its ability to promote crossing-over during meiosis. Genes Dev. **11:** 1573–1582.

Jeffreys, A. J., R. Neumann and V. Wilson, 1990 Repeat unit sequence variation in minisatellites: a novel source of DNA polymorphism for studying variation and mutation by single molecule analysis. Cell **60:** 473–485.

Jessop, L., T. Allers and M. Lichten, 2005 Infrequent co-conversion of markers flanking a meiotic recombination initiation site in *Saccharomyces cerevisiae*. Genetics **169:** 1353–1367.

Kearney, H. M., D. T. Kirkpatrick, J. L. Gerton and T. D. Petes, 2001 Meiotic recombination involving heterozygous large insertions in *Saccharomyces cerevisiae*: formation and repair of large, unpaired DNA loops. Genetics **158:** 1457–1476.

Mazina, O. M., A. V. Mazin, T. Nakagawa, R. D. Kolodner and S. C. Kowalczykowski, 2004 *Saccharomyces cerevisiae* Mer3 helicase stimulates 3′–5′ heteroduplex extension by Rad51: implications for crossover control in meiotic recombination. Cell **117:** 47–56.

McKee, A. H., and N. Kleckner, 1997 A general method for identifying recessive diploid-specific mutations in *Saccharomyces cerevisiae*, its application to the isolation of mutants blocked at intermediate stages of meiotic prophase and characterization of a new gene *SAE2*. Genetics **146:** 797–816.

Merker, J. D., M. Dominska and T. D. Petes, 2003 Patterns of heteroduplex formation associated with the initiation of meiotic recombination in the yeast *Saccharomyces cerevisiae*. Genetics **165:** 47–63.

Nag, K. K., M. A. White and T. D. Petes, 1989 Palindromic sequences in heteroduplex DNA inhibit mismatch repair in yeast. Nature **340:** 318–320.

Porter, S. E., M. A. White and T. D. Petes, 1993 Genetic evidence that the meiotic recombination hotspot at the *HIS4* locus of *Saccharomyces cerevisiae* does not represent a site for a symmetrically processed double-strand break. Genetics **134:** 5–19.

Prinz, S., A. Amon and F. Klein, 1997 Isolation of *COM1*, a new gene required to complete meiotic double-strand break-induced recombination in *Saccharomyces cerevisiae*. Genetics **146:** 781–795.

Prolla, T. A., D.-M. Christie and R. M. Liskay, 1994 Dual requirement in yeast DNA mismatch repair for *MLH1* and *PMS1*, two homologs of the bacterial *mutL* gene. Mol. Cell. Biol. **14:** 407–415.

Sambrook, J., E. F. Fritsch and T. Maniatis, 1989 *Molecular Cloning: A Laboratory Manual*. Cold Spring Harbor Laboratory Press, Cold Spring Harbor, NY.

Schultes, N. P., and J. W. Szostak, 1990 Decreasing gradients of gene conversion on both sides of the initiation site for meiotic recombination at the *ARG4* locus in yeast. Genetics **126:** 813–822.

Sokal, R. R., and F. J. Rohlf, 1995 *Biometrics*. W. H. Freeman, San Francisco.

Southern, E. M., 1975 Detection of specific sequences among DNA fragments separated by gel electrophoresis. J. Mol. Biol. **98:** 503–517.

Surtees, J., J. Argueso and E. Alani, 2004 Mismatch repair proteins: key regulators of genetic recombination. Cytogenet. Genome Res. **107:** 146–159.

Szostak, J. W., T. L. Orr-Weaver, R. J. Rothstein and F. W. Stahl, 1983 The double-strand-break repair model for recombination. Cell **33:** 25–35.

Wach, A., A. Brachat, R. Pohlmann and P. Philippsen, 1994 New heterologous modules for classical or PCR-based gene disruptions in *Saccharomyces cerevisiae*. Yeast **10:** 1793–1808.

Worth, L., Jr., S. Clark, M. Radman and P. Modrich, 1994 Mismatch repair proteins MutS and MutL inhibit RecA-catalysed strand transfer between diverged DNAs. Proc. Natl. Acad. Sci. USA **91:** 3238–3241.

Worth, L., Jr., T. Bader, J. Yang and S. Clark, 1998 Role of MutS ATPase activity in MutS, L-dependent block of in vitro strand transfer. J. Biol. Chem. **273:** 23176–23182.

Communicating editor: M. Lichten